A 140GHz Two-Channel CMOS Transmitter using Low-Cost Packaging Technologies

Arda Simsek, Ahmed S. H. Ahmed, Ali A. Farid, Utku Soylu and Mark J. W. Rodwell

ECE Department, University of California, Santa Barbara, CA 93106, USA
ardasimsek@ece.ucsb.edu

***Abstract*— We report a 2-channel 140GHz transmitter using low-cost antenna and packaging technologies. The arrays use 8-element series-fed linear microstrip patch antenna arrays fabricated on an Isola Astra MT77 printed circuit board (PCB). Two such antennas, connected to a CMOS multi-channel transmitter IC with 2dBm output power form the two-channel transmitter. At 145GHz, the measured transmitter EIRP is 14-15dBm in single-channel operation and 19-20dBm in two-channel operation. QPSK transmission experiments over 25 cm distance show open eye patterns at 10.0 Gb/s rates.**

Keywords—Millimeter wave integrated circuits, transceivers, transmitters, CMOS, SOI, phased arrays, MIMO, antennas, wirebonding transition.

I. Introduction

The rapid increase in data consumption creates a need for high-data-rate wireless links. Millimeter waves provide broad available spectrum, supporting high-data-rate wireless communications. Although (λ^2/R^2) and foul-weather attenuation are both are high, phased arrays can recover signal strength [1]. Given the short wavelengths, many antennas can be placed in a small aperture area, supporting many independent simultaneous beams (massive MIMO). To realize such complex systems, low-cost, high-yield technologies are critical. For this, CMOS is attractive, and several CMOS transceivers operating above 100GHz have been reported [2,3].

There is still the need for low-cost yet efficient and high-gain antennas and low-cost assembly techniques at these frequencies. Many published mm-wave systems have used on-chip antennas [4] with limited gain and efficiency, or wafer probing [5] to demonstrate data transmission. Importantly, recent work demonstrated low-loss Cu-stud flip-chip IC-antenna interconnection above 100GHz [6]. Such assembly provides low IC-package interconnect losses but requires tighter lithographic resolution in the package design.

This work integrates two previous results. In [7], we reported at 140GHz CMOS 4-channel multi-channel transmitter and 4-channel receiver. In [8], we demonstrated integration of these ICs with low-cost PCB antennas, demonstrating both the efficacy of PCB patch antennas and the performance of low-cost ball-bonding at 140GHz. Here we demonstrate a two-channel transceiver, and show spatial power-combining. The transmitter antenna array has two elements with separate electrical feeds, each element being a series-fed microstrip patch antenna array. The linear array antennas are separated by ~0.5λ (1.1mm) to allow steering over wide angles without grating lobes.

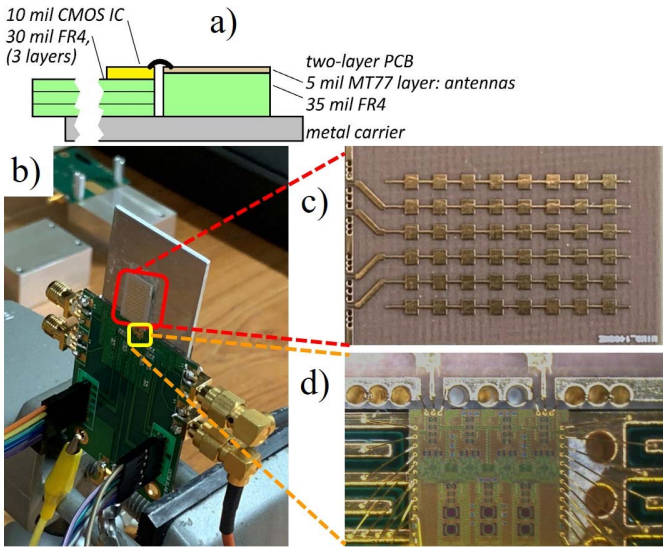

Figure 1: Two-channel transmitter integrating a CMOS transceiver IC, a PCB carrying a microstrip patch antenna array, and a second PCB carrying low-frequency connections to the IC. (b) Zoomed image showing the ICs and wire-bond interface. (c) PCB 4-element antenna array, each of which is an 8-element series-fed linear microstrip patch antenna array. (d) Magnified image showing the wire-bonds. (e) Schematic cross-section of the assembly.

II. Transmitter IC

The 4-channel transmitter, on a 1.67mm × 1.76mm die, was previously reported in [7]. 9:1 frequency multiplier chains generate the ~140GHz local oscillator from a ~15.5GHz input. The baseband (I, Q) inputs are directly mixed against the 140GHz LO, summed and amplified to form the 140GHz transmitter output. Only two of the four channels are used in this experiment due to the density of wirebond interconnects. At 140GHz, the transmitter saturated output power is -2dBm with a 1V supply and 2dBm with the 1.1V supply (Figure 2). The 3-dB bandwidth is greater than 15GHz.

III. Antenna Design and Measurements

The antenna design was previously reported in [8]. An 8-element 144GHz series-fed microstrip patch antenna array was fabricated on a printed circuit board material, Isola Astra-MT77, (ε_r=3, tanδ=0.0017), and fabricated in a low-cost PCB technology with 3mil minimum resolution and 5mil substrate thickness. The PCB is a two-layer laminate with a 35mil FR4 under the MT77 layer. The combined thickness of the MT77 and FR4 layers is equal to the combined thickness of the

978-1-7281-5178-6/20/$31.00 ©2020 IEEE

CMOS IC and the FR4 board on which it is mounted (Figure 1e). Bond pads on the CMOS IC and on the antenna PCB are therefore at equal height, minimizing wire bond length. Series-fed microstrip patch antenna arrays are designed and simulated (Ansys HFSS) using the procedures in [9], with a quarter wavelength transformer matching the antenna array input to 50Ω. Anticipating that simulated and measured antenna resonant frequencies might differ, antennas were fabricated with designed resonant frequencies of 136, 140, and 144GHz.

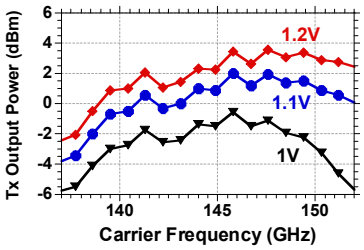

Figure 2: Transmitter output power as a function of frequency and supply voltage

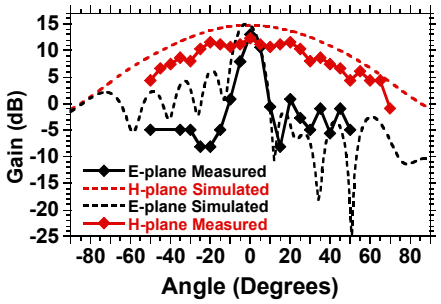

Figure 3: Simulated (144 GHz) and measured (148 GHz) E-plane and H-plane radiation patterns of the 144GHz series-fed patch array.

Antenna gain was measured using a small-scale antenna test range with diode multipliers as signal sources and diode harmonic mixers as signal detectors [8]. Figure 3 compares the simulated (at 144GHz) and measured (at 148GHz) E-plane and H-plane radiation patterns. The peak antenna gain, at ~13.6 dB, is 1.5-2 dB smaller than simulated. The measured bandwidth is 7GHz. We ascribe the ~4GHz frequency shift between measurement and simulation to lithographic linewidth variations in the PCB manufacturing.

IV. Wirebonding Compensation and Transition Design

Design of the wire-bond transition between the antenna and the 140GHz CMOS transmitter output was previously reported in [8]. The board thicknesses were selected such that the height of the antenna and the CMOS pads are aligned within +/- 50µm accuracy, and in assembly, the gap between the CMOS carrier PCB and the antenna PCB distance is kept below 50 µm (Figure 1). This permits a 0.3mm wire bond length, giving 250-300pH inductance. The CMOS IC signal pads are ground-signal-ground, hence the antenna PCB substrate provides vias connecting the microstrip ground plane to ground pads which are bonded to the CMOS IC ground pads. The vias add additional series inductance. The IC-PCB transition incorporates as a series tuning element to tune these transition parasitics, and the simulated transition loss is 1.8dB. Though this transition loss has not been experimentally verified by direct measurement, the measured single-channel transmitter radiated output power is consistent with the measured CMOS transmitter output power, the antenna gain, and the simulated transition loss [8].

V. Spatial Power-Combining Experiments

The transmitter IC and antenna array were wire-bonded together to form the transmitter of Figure 1. There are only two active transmitter channels. The transmitter was tested (Figure 4) by driving its inputs by data from an arbitrary waveform generator (AWG), and by measuring the radiated power with a standard-gain horn coupled to a harmonic mixer and spectrum analyzer. The spectrum analyzer and harmonic mixer sensitivity was calibrated using a 140GHz test signal source and a mm-wave power meter. From the measured received power, the known gain of the standard-gain horn, and the transmitter-receiver separation distance, the transmitter EIRP can then be measured.

If the AWG generates quadrature single-tone inputs for (I, Q) inputs of one transmitter channel, then the transmitter will generate single-sideband modulation. If both transmitter channels are driven in this fashion, adjusting the relative phases of the transmitter inputs will adjust the relative phases of the transmitter outputs. Bringing the two transmitter outputs into phase (Figure 5a) results in spatial power-combining of the two transmitters. The EIRP is then 19.9dBm.

If, instead, the first transmitter is driven with such single-sideband modulation, and the second transmitter is driven with constant (DC) baseband inputs, then the two transmitters will radiate at different frequencies, without spatial power-combining. In this case (Fig. 9b) the two transmitters have EIRP of 14.3dBm and 14.6dBm.

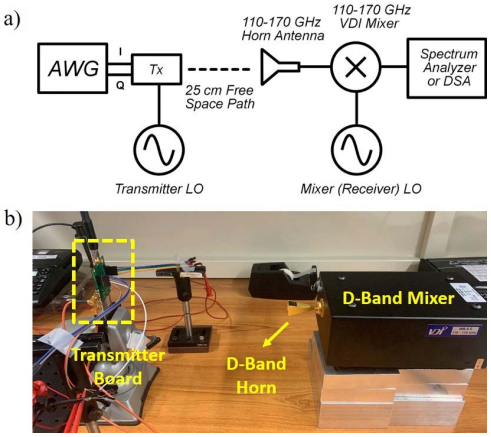

Figure 4: (a) Schematic diagram and (b) photograph of the apparatus for radiated power measurements and data transmission measurements.

The measurement is then repeated while sweeping the LO frequency. The result (Fig. 10) shows transmitter power-combining as a function of frequency. The observed EIRP is consistent, within experimental error, with the measured transmitter IC output power, the measured antenna gain, and the simulated wire-bond insertion loss.

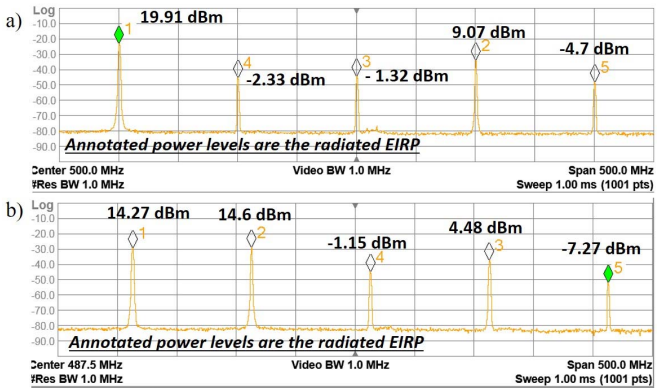

Figure 5: Received output spectra from the two-channel transmitter. In (a), both channels are driven with (I, Q) inputs corresponding single-sideband modulation with the two transmitters radiating in-phase. The measured EIRP is then 19.9dBm. This demonstrates spatial power-combining. In (b) one channel is driven with (I, Q) inputs corresponding single-sideband modulation, while the other transmitter operates with DC (I, Q) inputs. The two transmitters then radiate at different frequencies, with measured EIRP for the two tones of 14.3 and 14.6dBm.

VI. Conclusion

We have demonstrated two-channel power-combining on a 140GHz phased-array transceiver using CMOS ICs and a two-element series-fed linear microstrip patch antenna array fabricated on a low-cost PCB. The transmitter showed 20dBm EIRP, consistent to within measurement precision with the transmitter output power, simulated interface losses, and measured antenna gain. To our knowledge, this is the first work demonstrating the fully packaged multi-channel transmitter above 140GHz [4,6,10,11].

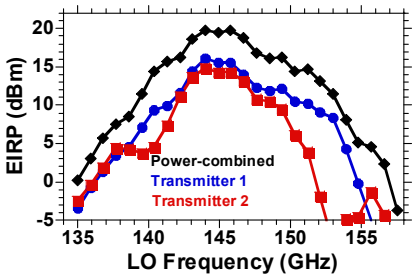

Figure 6: EIRP vs. frequency with the two transmitters power-combined and operating independently.

Acknowledgment

This work was supported by National Science Foundation (NSF) Giganets Program, Contract NO. CNS-1518812. The author would like to thank Global Foundries for the 45 nm CMOS SOI chip fabrication, and Advotech for the assembly. Authors also would like to thank Navneet Sharma, Hamidreza Memerzadeh, Nikolaus Klammer, and Gary Xu at Samsung Research America for valuable suggestions and the measurement equipment. Authors also would like to thank Mohammed Abdelghany, Maryam E. Rasekh, Prof. Upamanyu Madhow and Prof. James F. Buckwalter for valuable comments.

[1] S. Shahramian, M. J. Holyoak, and Y. Baeyens, "A 16-Element W-Band phased array transceiver chipset with flip-chip PCB integrated antennas for multi-gigabit data links," in Proc. Radio Freq. Integr. Circuits Symp., 2015, pp. 27-30.

[2] Ali A. Farid, Arda Simsek, Ahmed S. H. Ahmed, and Mark J. W. Rodwell "A Broadband Direct Conversion Transmitter/Receiver at D-Band UIsing CMOS 22nm FDSOI," . Radio Freq. Integr. Circuits Symp., 2019, in press

[3] S. Kang, S. V. Thyagarajan and A. M. Niknejad, "A 240 GHz Fully Integrated Wideband QPSK Transmitter in 65 nm CMOS," in IEEE Journal of Solid-State Circuits, vol. 50, no. 10, pp. 2256-2267, Oct. 2015.

[4] A. Visweswaran et al., "9.4 A 145GHz FMCW-Radar Transceiver in 28nm CMOS," 2019 IEEE International Solid-State Circuits Conference - (ISSCC), San Francisco, CA, USA, 2019, pp. 168-170.

[5] S. Carpenter et al., "A D-Band 48-Gbit/s 64-QAM/QPSK Direct-Conversion I/Q Transceiver Chipset," in IEEE Transactions on Microwave Theory and Techniques, vol. 64, no. 4, pp. 1285-1296, April 2016

[6] M. Sawaby, N. Dolatsha, B. Grave, C. Chen and A. Arbabian, "A Fully Packaged 130-GHz QPSK Transmitter With an Integrated PRBS Generator," in IEEE Solid-State Circuits Letters, vol. 1, no. 7, pp. 166-169, July 2018.

[7] A. Simsek, S. Kim and M. J. W. Rodwell, "A 140 GHz MIMO Transceiver in 45 nm SOI CMOS," 2018 IEEE BiCMOS and Compound Semiconductor Integrated Circuits and Technology Symposium (BCICTS), San Diego, CA, 2018, pp. 231-234.

[8] A. Simsek, S.-K. Kim, M. Abdelghany, A. S. H. Ahmed, A. A. Farid, U. Madhow, M. J. W. Rodwell, "A 146.7 GHz Transceiver with 5 GBaud Data Transmission using a Low-Cost Series-Fed Patch Antenna Array through Wirebonding Integration", to be presented, 2020 RF wireless week, 26-29 January, San Antonio, Texas.

[9] B. Rupakula, A. Nafe, S. Zihir, Y. Wang, T. Lin and G. Rebeiz, "63.5–65.5-GHz Transmit/Receive Phased-Array Communication Link With 0.5–2 Gb/s at 100–800 m and ± 50° Scan Angles," in IEEE Transactions on Microwave Theory and Techniques, vol. 66, no. 9, pp. 4108-4120, Sept. 2018

[10] A. Bhutani, B. Göttel, A. Lipp and T. Zwick, "Packaging Solution Based on Low-Temperature Cofired Ceramic Technology for Frequencies Beyond 100 GHz," in IEEE Transactions on Components, Packaging and Manufacturing Technology, vol. 9, no. 5, pp. 945-954, May 2019.

[11] W. Volkaerts, N. Van Thienen and P. Reynaert, "10.2 An FSK plastic waveguide communication link in 40nm CMOS," 2015 IEEE International Solid-State Circuits Conference - (ISSCC) Digest of Technical Papers, San Francisco, CA, 2015, pp. 1-3.